Takestan Institute of Higher Education

Available online at **http://UCTjournals.com**

UCT Journal of Research in Science, Engineering and Technology

UCT. J. Resea. Scien. Engineer.Techno. (UJRSET)

Volume 3,Issue3 ***16-26 (2015)*** *ISSN 2382-977X*

MLP Based Islanding Detection Using Histogram Analysis for Wind Turbine Distributed Generation

Hassan Ghadimi and Homayoun Ebrahimian

Department of Engineering, Ardabil Branch, Islamic Azad University, Ardabil, Iran
**corresponding author, E-mail: HOMAYOUN EBRAHIMIAN*

ABSTRACT

Due to increase distributed generations, Islanding is an important concern for these resources. Personnel and equipment safety issues are main reasons to detection of islanding. Several techniques based on passive and active detection schemes have been proposed previously. Although passive schemes have a large non-detection zone (NDZ), concerns have been raised about active methods because of their degrading effect on power quality. Reliably detecting this condition is regarded by many as an ongoing challenge because existing methods are not entirely satisfactory. This paper proposes a histogram analysis method using a Multi Layer Perceptron (MLP) Neural Network approach for islanding detection in grid-connected wind turbines. The main objective of the proposed approach is to reduce the NDZ and to maintain the output power quality unchanged. In addition, this technique can also overcome the problem of setting detection thresholds which is inherent in existing techniques. The method proposed in this study has a small non-detection zone and is capable of detecting islanding accurately within the minimum standard time. Moreover, for those regions which require better visualization, the proposed approach can serve as an efficient aid for better detecting grid-power disconnection.

Original Article:

Received:28 June2015
Accepted :24 Aug 2015
Published :30 Sep 2015

Keywords:
Signal histogram, MLP, distributed generation, islanding detection, non-detection zone

Introduction

Due to recent and ongoing technological, social, economic, and environmental pollution developments, distributed generation (DG) using renewable energy sources has become one of the main sources of power [1]. Distributed generation (DG) units have become more competitive against conventional centralized systems by successfully integrating new-generation technologies and power electronics. Hence, they have attracted many customers from the industrial, commercial, and residential sectors [2].

The total global installed wind capacity at the end of 2010 was 430 TWh annually, which is 2.5% of total global demand. Based on current growth rates, the World Wide Energy Association (WWEA) predicts that in 2015, a global capacity of 600 GW is possible. By the end of 2020, at least 1500 GW can be expected to be installed globally [3]. However, connecting wind turbines to distribution networks produces some problems, such as islanding [4].

Islanding is an undesirable situation because it poses a potentially dangerous condition for maintenance personnel and may cause damage to the DG and to loads in the case of unsynchronized grid reconnection due to the phase difference between the grid and the DG [5]. Therefore, avoidance of islanding has become a mandatory feature in the IEEE Std.1547.1, IEEE Std.929-2000, and UL1741 standards [6].

Many techniques have been proposed to detect islands [7–9]. These techniques can be broadly classified into remote and local techniques. Remote techniques, including power-line signaling [10] and transfer trip [11], are based on communication between the utility and the DGs. Although these techniques may have better reliability than local techniques, they are expensive to implement and hence uneconomical.

Local techniques rely on information and data at the DG site and can be classified into active and passive techniques [12]. Passive-detection methods are based on measuring and analyzing certain system parameters [13]. Over/under voltage and frequency detection are among the simplest passive methods used in islanding detection. Unfortunately, if the load and the generation on the island are closely matched, the change in voltage and frequency might be very small and within thresholds, thus leading to an undetected islanding situation [14]. Other passive techniques have been proposed based on monitoring the rate of change of frequency (ROCOF) [15], phase-angle displacement [16], or the rate of change of generator power output [2], as well as impedance monitoring, the total harmonic distortion (THD) technique [13], and the wavelet transform function [17–19]. These offer superior sensitivity because their settings permit detection to take place within statutory limits, but these settings must be carefully selected to avoid malfunction during network faults. The tradeoff between the two performance criteria is especially difficult for these methods. If the threshold for permissible disturbance in the quantities monitored is set to a low value, then nuisance tripping becomes an issue, and if the threshold is set too high, islanding may not be detected.

In active methods, the main theme is to design control circuits so that the required variations can be produced at the outputs of the distributed generators [20]. Then, once loss of grid power takes place, this designated bias will accordingly enlarge sufficiently to trip the connected relays, thus signaling occurrence of the event. On the contrary, when the utility supply is operating normally, the amount of variation will be insufficient to trip the relays, ensuring that no event misidentification takes place. The main advantage of active techniques over passive techniques is their small NDZ [21]. Some important active techniques are impedance measurement, frequency shift, and automatic phase drift [22], current injection [5], Sandia frequency shift and Sandia voltage shift [21], and negative phase-sequence current injection [24]. These active methods require a complex circuit controller for detection and are also used for inverter-based distributed generation or synchronous generators. Power-quality problems are another disadvantage of active methods.

This paper introduces a passive islanding-detection method based on histogram and MLP approach to detect islanding in wind-turbine systems. The main advantage of the histogram-based approach is to reduce the NDZ and to maintain the output power quality unchanged. In addition, this technique can also overcome the problem of setting detection thresholds using a MLP technique. Using this approach, an islanding situation can be detected accurately within the minimum standard time. The highlights of the proposed method can be summarized as follows:

- Small non-detection zone
- Capable to use for uncontrolled distributed generation
- Easy and inexpensive implementation
- Does not need a threshold value.

The proposed method is applied to a self-excited wind-turbine system, and the advantages are verified.

2. Case Study

Figure 1 shows a single-line diagram of the proposed islanding-detection system. The self-excited wind-turbine induction generator is the DG unit, which has a rated voltage of 0.69 kV and is connected to a point of common coupling (PCC) using a step-up transformer with rated power of 1 MVA. The local load is a three-phase parallel RL before the circuit breaker (CB), in which "*r*" stands for the series resistance inductance and R_L is the parallel load connected to the system by a Y connection. A capacitor bank is used for power-factor correction. Local load and system parameters are given in Table 1. At first, the system is operated in the grid-connected condition; the islanding mode occurs when the CB is open. For evaluation of islanding-detection techniques, the parallel R_L is traditionally used as the local load when the load inductance is adjusted to the system frequency.

Note that the DG frequency and voltage should have admissible values in both grid-connected and islanded modes. In the grid-connected condition, the voltage magnitude and frequency of the local load at the PCC are regulated by the grid.

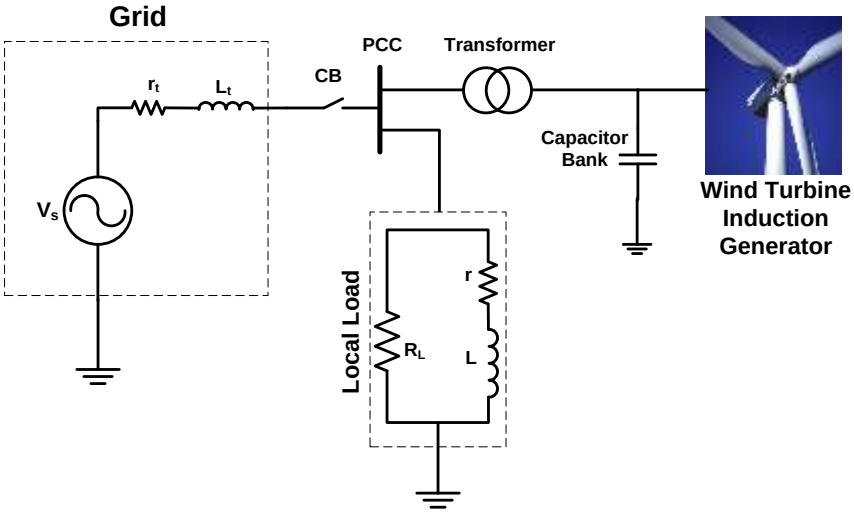

Fig. 1: Single-line diagram of study system.

Table 1: Parameters of study system

DG nominal power	660 KVA
$Voltage_{rms}$ (L-L)	690 V
r_s	0.5269 Ω
L_s	17.1 mHz
Nominal frequency	50 Hz
R	2667 Ω
L	2.37 H
C	1.592 **μ**F

3. Transfer Function of Islanded System

This section describes the state-space mathematical model of the islanded system [2]. In the island condition, a simple circuit model of a self-excited induction generator with fixed wind speed is shown in Fig. 2. It is assumed that the DG unit and the local load are balanced three-phase subsystems within the island.

For such subsystems within the island, the state-space model is:

$$\begin{cases} v_g^{abc}(t) = L_s \dfrac{di_g^{abc}(t)}{dt} + r_s i_g^{abc}(t) + v_t^{abc}(t) \\ i_g^{abc}(t) = i_m^{abc}(t) + C\dfrac{dv_t^{abc}(t)}{dt} + \dfrac{1}{R_L} v_t^{abc}(t) \\ v_t^{abc}(t) = L_m \dfrac{di_m^{abc}(t)}{dt} + r_m i_m^{abc}(t) \end{cases} . \quad (1)$$

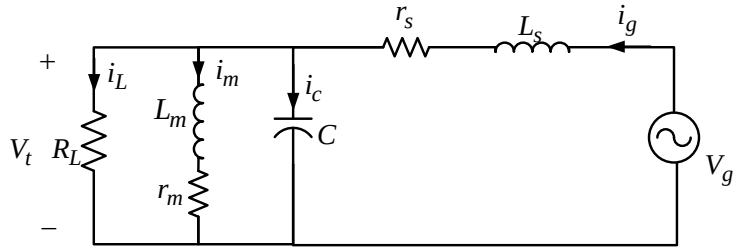

Fig. 2: Simple model of case study.

In the $\alpha\beta$ frame, the dynamic model of the system is:

$$\begin{cases} v_g^{\alpha\beta}(t) = L_s \dfrac{di_g^{\alpha\beta}(t)}{dt} + r_s i_g^{\alpha\beta}(t) + v_t^{\alpha\beta}(t) \\ i_g^{\alpha\beta}(t) = i_m^{\alpha\beta}(t) + C\dfrac{dv_t^{\alpha\beta}(t)}{dt} + \dfrac{1}{R_L} v_t^{\alpha\beta}(t) . \\ v_t^{\alpha\beta}(t) = L_m \dfrac{di_m^{\alpha\beta}(t)}{dt} + r_m i_m^{\alpha\beta}(t) \end{cases} \quad (2)$$

By transferring these equations to a rotated reference frame ($x_{\alpha\beta} = x_{dq} e^{j\theta}$) and assuming constant frequency in the islanded condition, the ABCD matrices of the state-space equation with $x = \begin{bmatrix} i_{gd} & i_{gq} & v_{td} & v_{tq} \end{bmatrix}^T$ can be written as follows:

$$A = \begin{bmatrix} -\dfrac{r_s}{L_s} & \omega_0 & 0 & -\dfrac{1}{L_s} \\ \omega_0 & -\dfrac{r_m}{L_m} & -2\omega_0 & \dfrac{CR_L\omega_0 r_s - L_m\omega_0}{L_m R_L} \\ 0 & \omega_0 & -\dfrac{r_m}{L_m} & \dfrac{1}{L_m} - \omega_0^2 C \\ \dfrac{1}{\mathrm{C}} & 0 & -\dfrac{1}{\mathrm{C}} & \dfrac{1}{CR_L} \end{bmatrix}, \quad (3)$$

$$B = \begin{bmatrix} \dfrac{1}{L_s} & 0 & 0 & 0 \end{bmatrix}^T, C = \begin{bmatrix} 0 & 0 & 1 & 0 \end{bmatrix}, D = 0$$

Finally, assuming $V_d(s) = Y(s)$, the transfer function of the state-space model is given by:

$$V_{td}(s) = \frac{(1.5s^2 + 15.63s + 14790)e4}{(4.0e-4)s^4 + 1.359s^3 + 1.542e4s^2 + 6.266e5s + 1517e6} \quad (4)$$

The step response of the output voltage is plotted in Fig. 3.

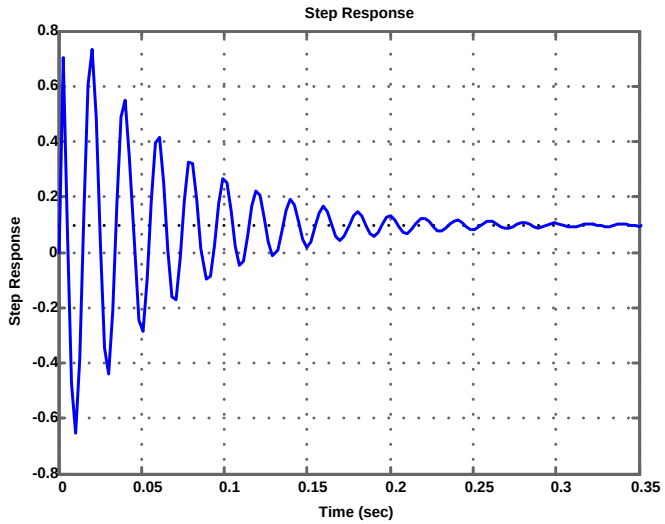

Fig. 3. Step response of $V_{td}(s)$ for the case study.

From Fig. 3, the transient response time is about 0.2 seconds; 0.2 second is therefore assumed as the analysis time to achieve reliable detection of the step response.

4. Non-Detection Zone (NDZ)

To determine the performance of an islanding detection method, the size of the non-detection zone (NDZ) is one of the most important characteristics. The NDZ is defined as an operating region where islanding conditions cannot be detected in a timely manner. In this region, the power mismatch between production and consumption has a small value. In this part of the study, the NDZ was determined based on over/under voltage protection (OVP/UVP) and over/under frequency protection (OFP/UVP). The method was implemented using constant-current controlled inverters. To determine the amount of mismatch for which the OVP/UVP and OFP/UFP will fail to detect islanding, the amount of active power mismatch can be expressed in terms of load resistance as follows:

$$\Delta P = 3 \times V \times I - 3 \times (V + \Delta V) \times I = -3 \times \Delta V \times I \,, \quad (5)$$

Where, V and I represent the rated voltage and current respectively. An acceptable voltage range in a distribution network is between 0.88 pu and 1.1 pu. These voltage levels are equivalent to $\Delta V^{pu} = -0.12$ and $\Delta V^{pu} = 0.1$ respectively. The calculated imbalance amounts for the test network under study according to Eq. (14) (the output power under match conditions is 150 kW) are 18 kW and -15 kW respectively. The frequency and voltage of an RLC load have active and reactive power as follows:

$$P_L = \frac{V_t^2}{R_L}, \quad (6)$$

$$Q_L = V_t^2 \left(\frac{1}{\omega L_m} - \omega C \right), \quad (7)$$

where ω, P, and Q are the load frequency, active power, and reactive power respectively. In a grid-connected condition, the PCC voltage of is dictated by the main grid. Once the island has become established, the PCC voltage deviation leads to an active power imbalance with the nominal values. Because the output power of the inverter is at unity power factor, before islanding, the reactive power of the load is supplied entirely by the network, and after islanding, the amount of reactive power imbalance is equal to the consumed load before islanding; hence, it is possible to write:

$$\Delta Q = 3\frac{V_t^2}{\omega_n L_m}\left(1 - \omega^2 L_m C\right) = 3\frac{V_t^2}{\omega_n L_m}\left(1 - \frac{\omega_n^2}{\omega_r^2}\right), \quad (8)$$

where ω_n and ω_r are respectively the rated frequency and the resonance frequency of the load. If the resonance frequency is generated from unbalanced power, then the frequency change after the occurrence of islanding is equal to the difference between the network frequency and the load resonance frequency:

$$\omega_r = \omega_n \pm \Delta\omega \;, \omega_r = \frac{1}{\sqrt{L_m C}}. \quad (9)$$

Therefore, the reactive power imbalance needed for a certain change in frequency can be obtained as:

$$\Delta Q = 3\frac{V_t^2}{\omega_n L_m}\left(1 - \frac{f_n^2}{(f_n - \Delta f)^2}\right). \quad (10)$$

In this study, the acceptable frequency range was assumed to be between 49.7 and 50.3 Hz; these frequencies are equivalent to $\Delta f = -0.3$ and $\Delta f = 0.3$ Hz. Therefore, the values of reactive power imbalance are 6.393 kVAr and -6.51 kVAr respectively.

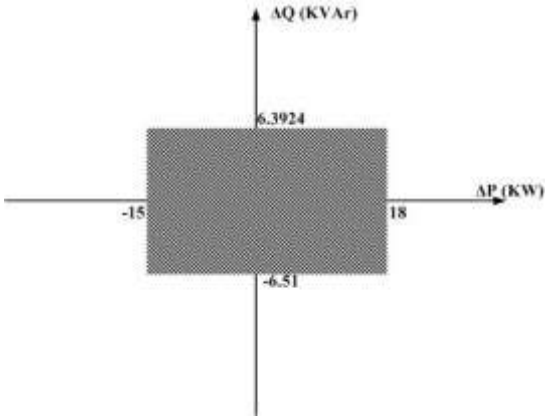

Fig. 4. NDZ for the constant-current interface controls for distributed generation.

5. PROPOSED ALGORITHM

This study proposes a histogram-based approach for islanding detection. To avoid having to specify thresholds, the ability of a MLP neural network to learn about the islanding condition will be combined with the algorithm.

5.1 Multi Layer Perceptron

The concept of the proposed technique is to recognize the sensitivity patterns of certain indices at a target location to specific credible events. The neural network technique is used to recognize and classify complex fault patterns. Many independent variables are defined with respect to this target location. A neural network consists of many simple neurons which are connected with each other. The feed-forward back-propagation Multilayer Perceptron (MLP) is the most standard neural classifier in pattern classification which widely used in fault patterns [25, 26].Also, MLP is useful to solve stochastic problems. Fig. 5 shows the integral structure of the MLP artificial neural network. The numbers of neuron in both input and output layer depend on the applied problem, while the number of neuron in the hidden layer is arbitrary and is usually decided by trial-and-error.

In classification problems, four activation functions are defined as:

- Linear activation function: The linear activation function for the entire real number range produces positive numbers and defined as:

$$\sigma(x) = ax + b \tag{11}$$

, which a and b are constant

- Logistic function: The logistic function is a common sigmoid curve, and scales input data to (0, 1) according to:

$$\sigma(x) = \left(1 + e^{-x}\right)^{-1} \tag{12}$$

- Softmax activation function: The softmax activation function scales all of the output vales between 0 and 1, and their sum is 1, which is a generalization of the logistic function to multiple variables.

$$\sigma(x) = \frac{e^{x}}{\sum e^{x}} \tag{13}$$

- Hyperbolic tangent activation function: The hyperbolic tangent function is defined as the ratio between the hyperbolic sine and the cosine functions and defined as (14).

$$\sigma(x) = \frac{e^{x} - e^{-x}}{e^{x} + e^{-x}} \tag{14}$$

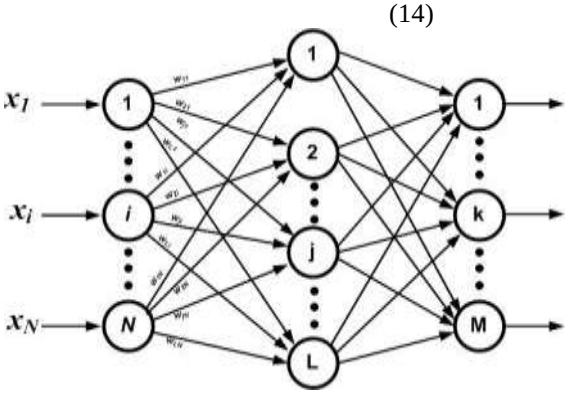

Fig. 5.MLP architecture

5.2 Specified Events

In this methodology, an extensive set of specified events is simulated offline to capture all of possible detection signal. These specified events are defined in the event database from which the network simulator executes the required events. In the next step, this database is used to initialize the MLP neural network learning machine. The definition of these events is based on Operational requirements in the IEEE1547 standards, Testing practices that are recommended by most manufacturers of islanding relays and Possible operating-network topologies.

The specified events are categorized into faults and switching actions under different network operating states. Some of the possible events are:

- All possible circuit-breaker trips which lead to island formation (at various loads between -135 kW and 168 kW)
- Opening of any breakers between the power system and the DG
- Abrupt change in the distributed generation load (35 kW to 80 kW)
- Loss of any lines in the distribution network
- Motor startup at various capacities (15–45 kW)
- Capacitor-bank switching at various capacities (15–50 kVAr)
- Nonlinear load switching to the network (15–50 kW).

A. Tasks of the Methodology

5.3 Applied MLP in Proposed Relay

In this paper, MLP classifier with three layers is exploited in classifying Islanding condition of wind turbines. The selected histogram of active and reactive power ($H=[h_1 \quad h_2 \quad ... \quad h_N]$), which n is the dimension of histogram vector, is applied to the input layer. In the hidden layer, $W^{in}=[w_{11}^{in} \quad ... \quad w_{ji}^{in} \quad ... \quad w_{LN}^{in}]$, $1\le i\le N$, $1\le j\le L$, is the input weight vector of the hidden layer and L is the number of neurons in the hidden layer. The output weight vector of the hidden layer is $W^{out}=[w_{11}^{out} \quad ... \quad w_{kj}^{out} \quad ... \quad w_{ML}^{out}]$, $1\le k\le M$ which, M is the number of output neurons. In three layers, σhid and σout are the activation transfer function in hidden and output layers, respectively.

Our designed MLP structure is composed of one hidden layer. The number of neurons of input, hidden and output layers is 30, 15 and 1, respectively. The hyperbolic tangent and logistic activation function is adopted in the hidden layer and the output layer, respectively. Levenberg–Marquardt (LM) [27] algorithm, is one of the most efficient training algorithms of MLP, which is used for training in this classification problem. The output unit is connected to the tripping unit of the DG circuit breaker. If islanding is detected, the output of this unit is 1. Conversely, if islanding is not detected, the output of this unit is 0.

At First, the events were represented by the simulated system, and all possible signals were measured. Second, histogram analysis of these signals was performed. Next, from the histogram database signals, the best signals for islanding-condition detection were chosen. These selected data must contain both islanding and non-islanding (normal operation) information. Using the proposed method, the rates of change of active and reactive power-histogram signals was selected and plotted in Figs. 6 and 7. The next step was to perform subtractive clustering of the dataset and to construct a neural network system that could best predict the occurrence of islanding or normal conditions. After the training step, the NN machine is capable of detecting islanding and non-islanding conditions. Some of these situations are described in the next section. In the research described in this paper, the problem of setting thresholds for islanding-detection parameters has been overcome. The results obtained indicate that MLP is an effective method for islanding detection.

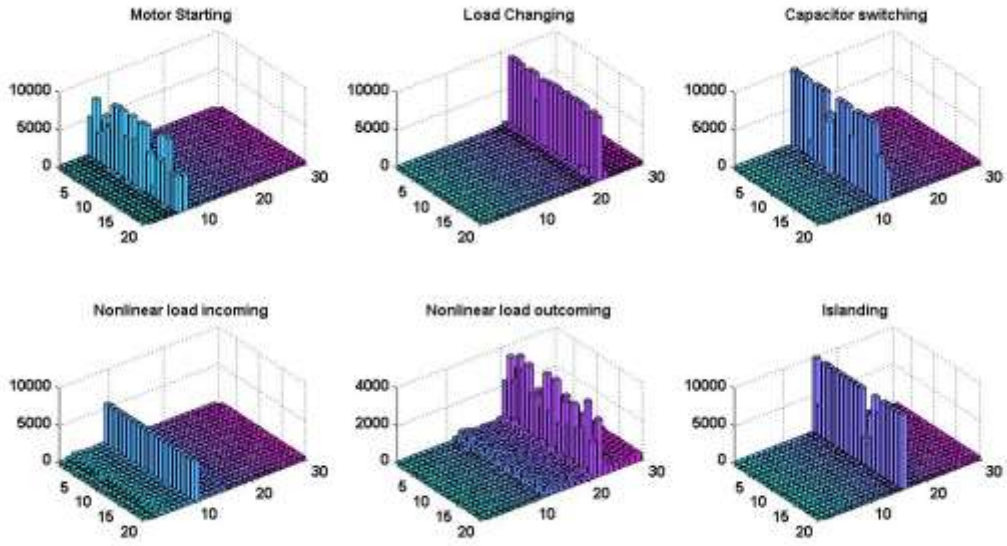

Fig. 6. Histogram of rate of change of active power signal.

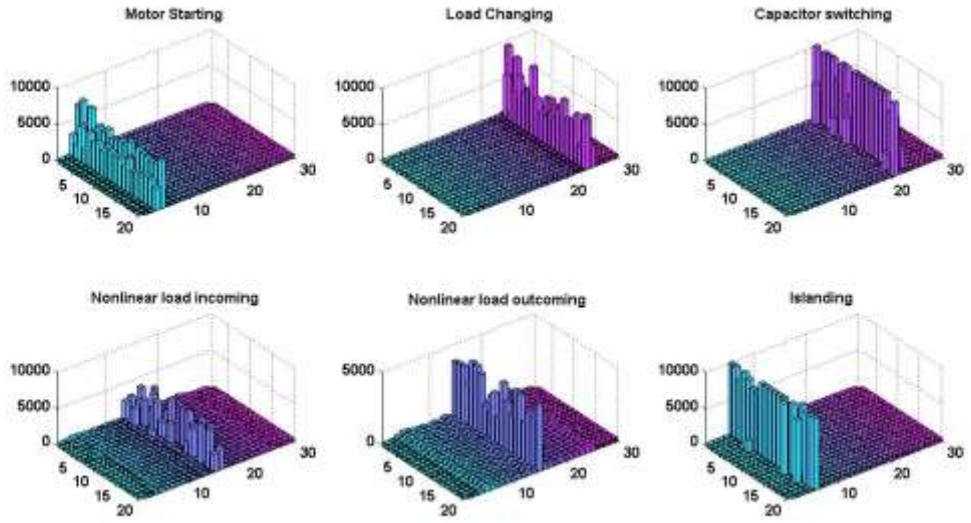

Fig. 7. Histogram of rate of change of reactive power signal.

6. Simulation Results

These sections describe learning in the MLP system and testing of the proposed islanding-detection relay under island operating conditions and in other switching situations.

6.1 Islanding Mode Test

In islanding operation mode, the performance of the proposed technique was verified for the various loading conditions given in Table 2. Selection of local loads should be such that the imbalance of reactive power is equal to zero. Under these conditions, island-mode detection is more difficult than in other situations. Furthermore, the load quality factor is equal to 1.8, which is the maximum recommended value in the standards.

For all conditions in Table 2, at t = 5 sec, the circuit breaker (CB) opened, isolating the wind turbine along with its local loads from the power grid, at which point islanding mode occurred. The effective voltage waveforms of the common coupling point for each of the cases listed in Table 2 are shown in Fig. 8(a). The frequencies of common coupling-point voltage for all cases listed in Table 2 are shown in Fig. 8(b). Figures 9 and 10 show respectively the rate of change of the active and reactive power histogram signals for these cases. Finally, in Fig. 11, the outputs of the detection method for all studied cases are shown. The output results of the MLP detection system are also shown in Fig. 11. It is apparent that under all islanding conditions, the MLP system could detect islanding-mode operation within 0.2 seconds.

	Conditio n1	Conditio n2	Conditio n3	Conditio n4	Conditio n5
R	2898.5 Ω	2739.7 Ω	2597.5 Ω	2500 Ω	2425 Ω

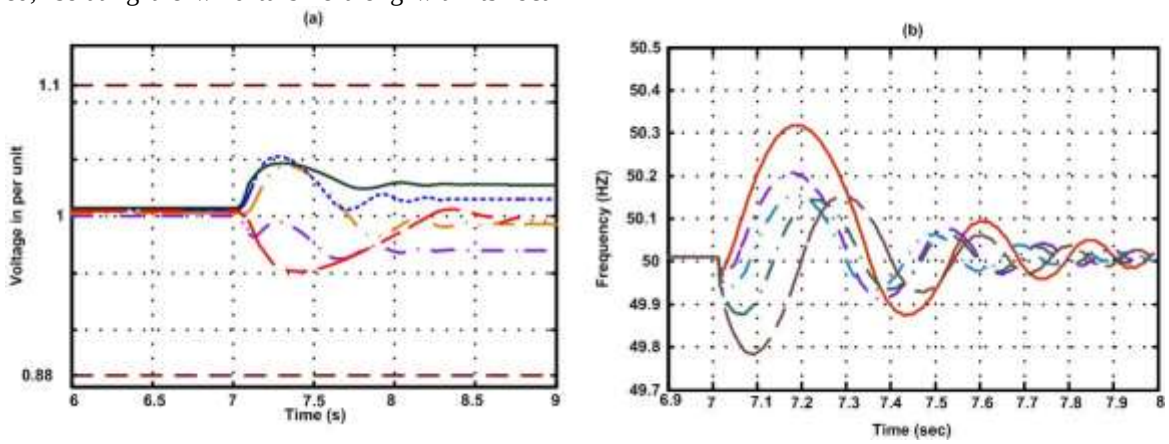

Fig. 8. a) Instantaneous value of PCC voltage; b) frequency of PCC voltage.

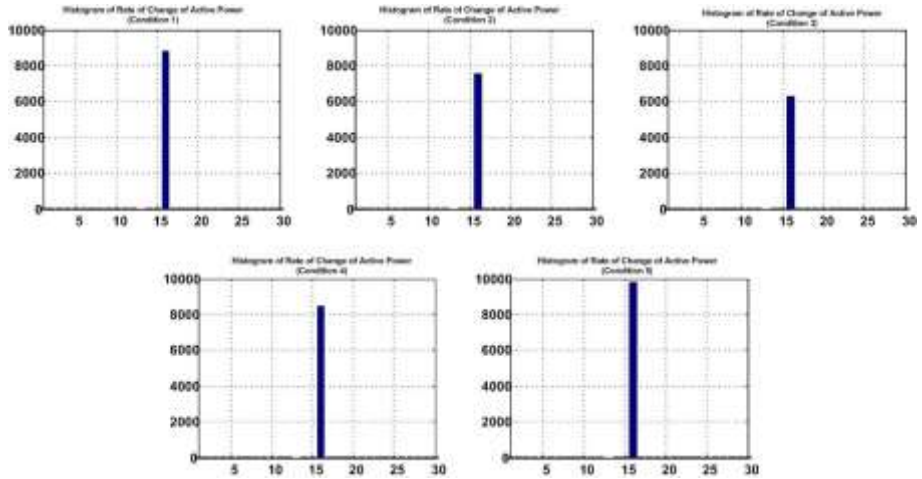

Fig. 9. Histogram of rate of change of active power.

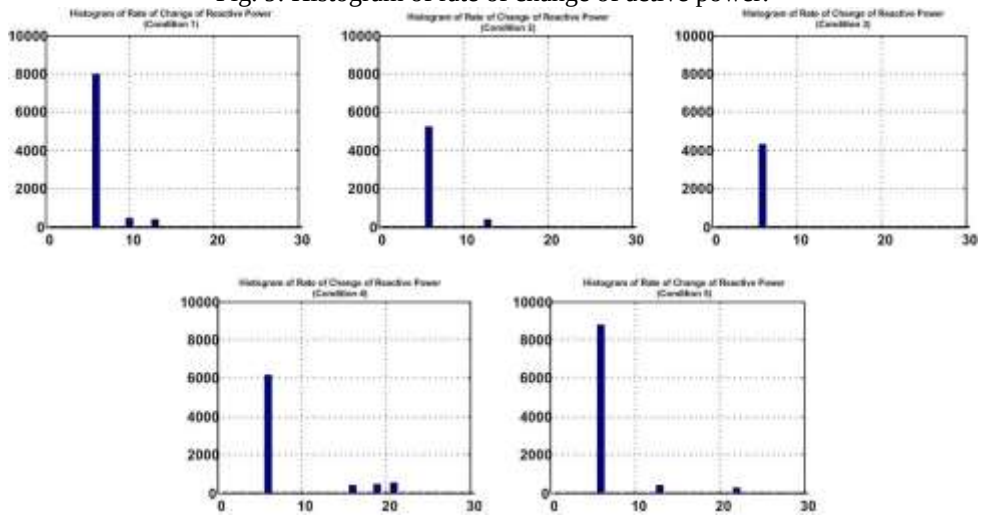

Fig. 10. Histogram of rate of change of reactive power.

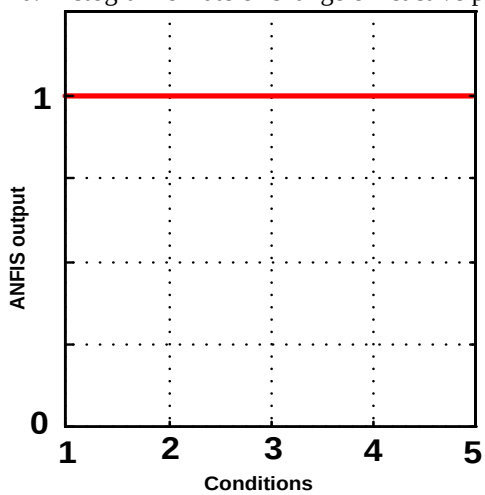

Fig. 11. MLP output for islanding situations.

B. Normal Operation

To show the performance of the proposed method, various conditions, such as motor, capacitor, linear and nonlinear load-switching results, were analyzed. The values of the various switching conditions are given in Table 3. For all examined cases in Table 3, switching at t = 5 s was applied to the system. Figure 12 shows the histogram of rate of change of active power and Fig. 13 the histogram of rate of change of

reactive power of the detection method for all studied cases. Figure 14 shows the results of the MLP system for all these switching conditions, indicating that the proposed algorithm could detect non-islanding conditions in all the situations studied.

Table 3: Non-islanding switching conditions

	Condition1	Condition2	Condition3	Condition4
Load Change	P=40 kW Q=20 kVAr	P=45 kW Q=25 kVAr	P=50 kW Q=25 kVAr	P=55 kW Q=30 kVAr
Motor Startup	P=20 kW Cosφ=0.78	P=25 kW Cosφ=0.78	P=30 kW Cosφ=0.78	P=40 kW Cosφ=0.78
Capacitor Switching	Q=15 kVAr	Q=20 kVAr	Q=25 kVAr	Q=30 kVAr
Nonlinear Load	P=8 kW	Q=15 kW	Q=20 kW	Q=30 kW

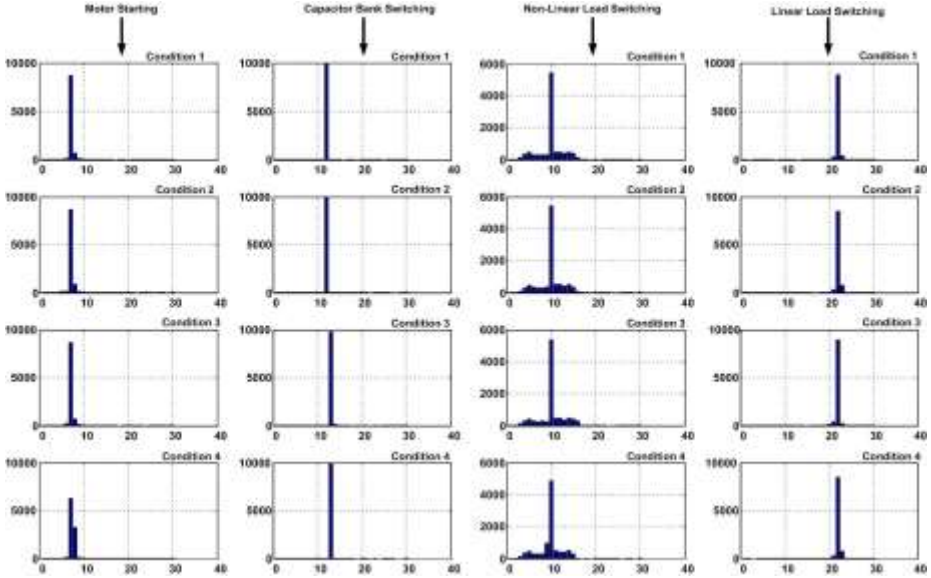

Fig. 12. Histogram of rate of change of active power signals in non-islanding situations.

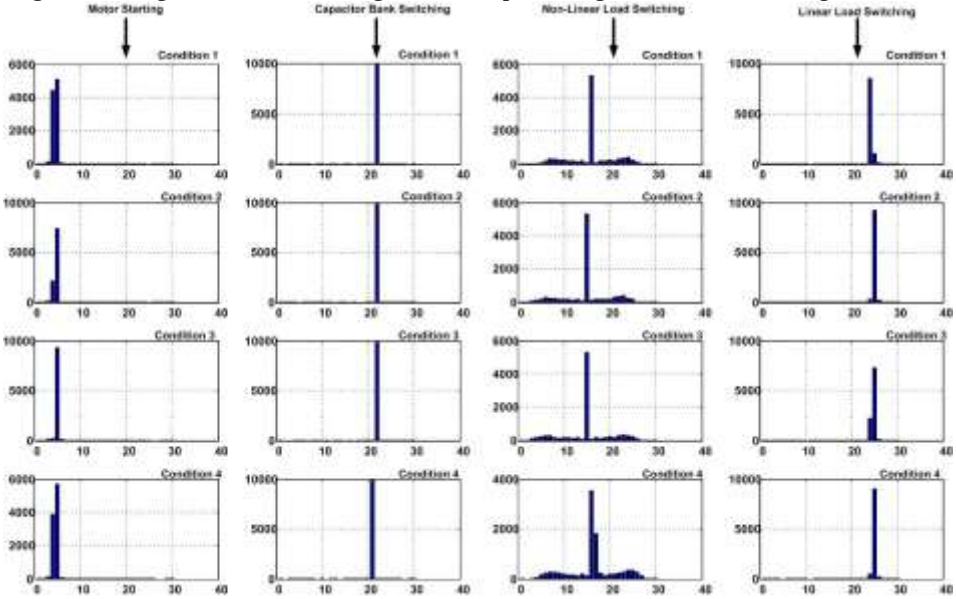

Fig. 13. Histogram of rate of change of reactive power signals in non-islanding situations.

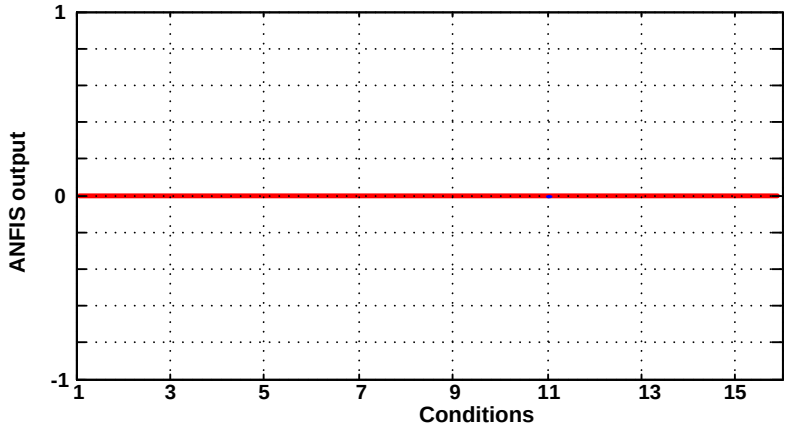

Fig. 14. Output of MLP detection system.

7. Conclusions

As a consequence of the increased number and size of wind-turbine units installed in a modern power system, protection against islanding has become extremely challenging. Islanding detection is also important because island operation of distributed systems is seen as a viable option in the future to improve the reliability and quality of the energy supply. Islanding situations must be prevented with distributed generation for safety reasons and to maintain the quality of power supplied to customers. A new histogram-based technique for islanding detection with distributed generation is proposed based on a neuro-fuzzy inference system. The main emphasis of the proposed scheme is to reduce the NDZ; in addition, this technique overcomes the problem of setting detection thresholds. This study proposes the use of a intelligent system called MLP for islanding detection. Using case studies with numerical conditions, the feasibility, flexibility, and robustness of the proposed approach were verified. Comparison of this histogram-based method with other islanding-detection methods during an islanding event with a negligible power imbalance showed that the proposed method works effectively for islanding detection in cases where other methods fail to detect islanding.

References:

[1] Kim, J.-H., Kim, J.-G., Ji, Y.-H., Jung, Y.-C., and Won, C.-Y., An islanding detection method for a grid-connected system based on the Goertzel algorithm, IEEE Trans. Power Electron., 26(4), 1049–1055 (2011).

[2] Hashemi, F., Ghadimi, N., Sobhani, B., Islanding detection for inverter-based DG coupled with using an adaptive neuro-fuzzy inference system, Electrical Power and Energy Systems 45: 443–455 (2013).

[3] Kazemi Karegar, H., Sobhani, B., Wavelet transform method for islanding detection of wind turbines, Renewable Energy 38: 94–106 (2012).

[4] Lidula, N.W.A., Rajapakse, A.D., A pattern-recognition approach for detecting power islands using transient signals—Part II: Performance evaluation, IEEE Trans. Power Deliv., 27(3), 1071–1080 (2012).

[5] Hernández-González, G., Iravani, R., Current injection for active islanding detection of electronically interfaced distributed resources. IEEE Trans. on Power Deliv., 21(3):1698–1705 (2006).

[6] Inverters, Converters, and Controllers for Use in Independent Power Systems, UL Std. 1741, 2002.

[7] Chiang, W.-J., Jou, H.-L., Wu, J.-C., Active islanding detection method for inverter-based distribution generation power system, Electrical Power and Energy Systems, 42: 158–166 (2012).

[8] Jou, H.-L., Chiang, W.-J., and Wu, J.-C., Virtual inductor-based islanding detection method for grid-connected power inverter of distributed power generation system, IET Renew. Power Gener., 1(3): 175–181 (2007).

[9] Velasco, D., Trujillo, C., Garcerá, G., Figueres, E., An active anti-islanding method based on phase-PLL perturbation,, IEEE Trans. Power Electron., 26(4): 1056–1066 (2011).

[10] Xu, W., Zhang, G., Li, C., Wang, W., Wang, G., Kliber, J., A power line signaling-based technique for anti-islanding protection of distributed generators—Part I: Scheme and analysis [a companion paper submitted for review].

[11] Mak, S.T., A new method of generating TWACS-type outbound signals for communication on power distribution networks, IEEE Trans. Power App. Syst., PAS-103(8): 2134–2140 (1984).

[12] El-Arroudi, K., Joós, G., Kamwa, I., McGillis, D.T., Intelligent-based approach to islanding detection in distributed generation, IEEE Trans. Power Deliv., 22(2), 828-835 (2007).

[13] Kazemi Karegar, H., Shataee, A., Islanding detection of wind farms by THD, IEEE Conf. DRPT2008, Nanjing, China: 6–9 (2008). Digital Code: 978-7-900714-13-8/08/_2008 DRPT.

[14] Chowdhurya, S.P., Chowdhury, S., Crossley, P.A., Islanding protection of active distribution networks with renewable distributed generators: A comprehensive survey, Electric Power Systems Research, [Ed.: volume and issue?] 1–9 (2009).

[15] Bright, C.G., COROCOF: comparison of rate of change of frequency protection: a solution to the detection of loss of mains, Proceedings, Developments in Power System Protection Conference, Publication No. 479, IEE Press, 2001.

[16] Best, R.J., Morrow, D.J., McGowan, D.J., Crossley, P.A., Synchronous islanded operation of a diesel generator, IEEE Trans. Power Syst., 2(4): 2170–2176 (2007).

[17] Ray, P.K., Mohanty, S.R., Kishor, N., Disturbance detection in grid-connected distributed generation system using wavelet and S-transform, Electric Power Systems Research, 81: 805–819 (2011).

[18] Dash, P.K., Padhee, M., Panigrahi, T.K., A hybrid time-frequency approach-based fuzzy logic system for power island detection in grid-connected distributed generation, Electrical Power and Energy Systems, 42: 453–464 (2012).

[19] Ukil, A., Zivanovíc, R., Abrupt change detection in power system fault analysis using adaptive whitening filter and wavelet transform, Electr. Power Syst. Res., 76: 815–823 (2006).

[20] Geng, H., Xu, D., Wu, B., Yang, G., Active islanding detection for inverter-based distributed generation systems with power control interface, IEEE Transactions on Energy Conversion, 26(4): 1063–1072 (2011).

[21] John, V., Ye, Z., Kolwalkar, A., Investigation of anti-islanding protection of power converter-based distributed generators using frequency domain analysis, Trans. Power Electron., 19(5): 1177–1183 (2004).

[22] Guo-Kiang, H., Chih-Chang, C., Chern-Lin, C., Automatic phase-shift method for islanding detection of grid-connected photovoltaic inverters, IEEE Trans. Energy Convers., 18(1): 169–173 (2003).

[23] Karimi, H., Yazdani, A., Iravani, R., Negative-sequence current injection for fast islanding detection of distributed resource unit. IEEE Trans. on Power Deliv., 23(1): 493–501 (2008).

[24] S.A.M. Javadian, M.-R. Haghifam, S.M.T. Bathaee, M. Fotuhi Firoozabad, Adaptive centralized protection scheme for distribution systems with DG using risk analysis for protective devices placement, Electrical Power and Energy Systems 44 (2013) 337–345

[25] Yu-Jen Lin, Comparison of CART- and MLP-based power system transient stability preventive control, Electrical Power and Energy Systems 45 (2013) 129–136

[26] A. Karami, S.Z. Esmaili, Transient stability assessment of power systems described with detailed models using neural networks, Electrical Power and Energy Systems 45 (2013) 279–292